Positronium collisions with molecular hydrogen

R. S. Wilde[1] and I. I. Fabrikant[2]
[1]*Department of Natural Sciences, Oregon Institute of Technology, Klamath Falls, Oregon 97601, USA*
[2]*Department of Physics and Astronomy, University of Nebraska, Lincoln, Nebraska 68588-0299, USA*
(Received 29 July 2015; published 14 September 2015)

Positronium (Ps) collisions with molecular hydrogen are investigated theoretically. Elastic and Ps ionization cross sections are calculated. For elastic scattering the pseudopotential method, previously developed for rare-gas atoms, is applied. Ps ionization cross sections are calculated using the binary-encounter approximation. The results agree with swarm measurements at low collision energies and with beam measurements at higher energies. The total Ps-H_2 cross section when plotted as a function of collision velocity is close to the e^--H_2 cross section at velocities above the Ps ionization threshold, confirming earlier observations [Brawley *et al.*, Science **330**, 789 (2010)]. However, below the threshold the two sets of cross sections are different because of the different nature of the long-range interaction between the projectile and the target, the polarization interaction in the case of e^--H_2 collisions and the van der Waals interaction in the case of Ps-H_2 collisions.

DOI: 10.1103/PhysRevA.92.032708 PACS number(s): 34.50.−s, 36.10.Dr, 82.30.Gg, 34.80.−i

I. INTRODUCTION

Positronium-atom and positronium-molecule collisions at low energies are mostly controlled by the electron exchange between the Ps electron and the target, and by the van der Waals interaction between the Ps and the target. Moreover, at energies above the Ps ionization threshold (6.8 eV) the exchange interaction becomes dominant. This, to a large extent, explains the recently discovered similarity [1–3] between e^- and Ps cross sections at intermediate energies when the cross section is plotted as a function of the projectile velocity. This similarity can also be explained, in a more direct way, within the framework of the impulse approximation [4]. However, the impulse approximation breaks down below the Ps ionization threshold; therefore, for a more accurate description of Ps scattering, methods that incorporate the Ps-target interaction are necessary [5].

Completely *ab initio* inclusion of electron exchange in Ps collisions with atoms and molecules is a very challenging task and has been accomplished only for simple targets such as the hydrogen atom [6,7]. Therefore it is advantageous to develop a simplified method of incorporating exchange in Ps collisions. A well-known method in electron collisions is based on the use of a local exchange potential derived from the free-electron gas model called the Hara free electron gas exchange (HFEGE) potential [8] and its modifications [9]. However, quite often the inclusion of this potential is not sufficient because this method does not provide the correct nodal structure of the wave function of the scattered electron. To satisfy the Pauli exclusion principle, the correct structure should guarantee the orthogonality of the wave function of the scattered electron to all occupied target orbitals. Therefore quite often the HFEGE potential is supplemented by the orthogonality constraints [10]. In many cases this procedure significantly improves agreement with the exact static-exchange calculations. For Ps-atom collisions the orthogonality condition was implemented by Biswas and Adhikari [11,12] in the form of an orthogonal exchange kernel similar to the exchange amplitude of Ochkur [13] and Rudge [14]. Integration of the static-exchange and close-coupling equations with these exchange kernels produces scattering cross sections for Ps collisions with rare-gas atoms that are in good agreement with existing experiments.

The orthogonality constraint can be mocked by introducing an l-dependent repulsive component in the effective potential for electron-atom or electron-molecule interaction [15]. The repulsive core makes the wave function of the scattered electron very small in the region where the occupied orbitals are significant, and therefore strongly reduces the overlap integral. This procedure reduces the actual scattering phase shift at low energies by a factor of π times an integer and leads to a violation of the Levinson-Swan theorem [16], but does not affect the cross sections at low energies. This approach leads to a description of the electron-target interaction in terms of an l-dependent pseudopotential [15].

It is particularly convenient for a description of Ps-atom scattering, since the orthogonality constraint is difficult to implement for the electron bound in Ps. The pseudopotential approach was successfully used [5] for theoretical description of Ps-Ar and Ps-Kr collisions. At higher energies, comparable to the energy of electronic excitation of the target, the pseudopotential approach starts to fail. However, if the excitation cross sections are not large, as in the case of the rare-gas atoms, the error might be not very significant. In the present paper we use the pseudopotential method to calculate elastic scattering of Ps by the hydrogen molecule. Since only one orbital, σ_g, is occupied in this case, we need to use the repulsive core only in one symmetry. We supplement the elastic cross-section calculations by calculation of ionization of Ps in Ps-H_2 collisions. As was shown in the atomic case [4,17], this is the major inelastic channel in Ps collisions; therefore the sum of elastic and Ps ionization cross sections produces the total cross section with good accuracy. In the next section we describe the basic theory, and then we present the results of our calculations and comparison with experiment. We note that since the discovery [1] of similarities between electron and Ps scattering, it became customary to plot the Ps scattering cross sections, as well as the electron cross sections, as functions of velocity rather than energy. We continue this tradition in the present paper. Atomic units are used throughout.

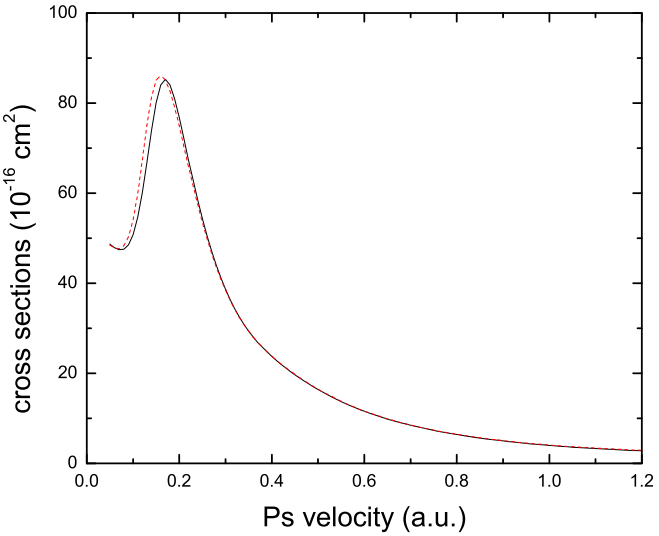

FIG. 1. (Color online) Elastic Ps-H_2 cross sections calculated by combining HFEGE and van der Waals potentials. Black solid line: only the spherically symmetric part of the potential is included. Red dashed line: the full anisotropic interaction is included.

II. THEORETICAL MODEL FOR PS-H_2 SCATTERING

A. Elastic scattering

The static contribution to the Ps-H_2 interaction is zero; therefore only the exchange potential contributes to Ps-H_2 scattering in the static-exchange approximation. The van der Waals interaction between Ps and H_2, accounting for the long-range part of electron correlation, can be written as

$$V_W(\mathbf{R}) = -\frac{C_0 + C_2 P_2(\cos\chi)}{R^6}\{1 - \exp[-(R/R_c)^8]\}, \quad (1)$$

where $\mathbf{R}$ is the position of the center of Ps relative to the center of H_2, χ is the angle between $\mathbf{R}$ and the internuclear axis, and R_c is a cutoff radius. The van der Waals coefficients C_0 and C_2 were calculated from the London formula [18] and the theoretical principal values of the polarizability tensor for H_2 [19], $\alpha_\parallel = 6.762$ a.u., $\alpha_\perp = 4.506$ a.u. These polarizabilities are related to α_0 and α_2 entering the polarization potential

$$V_{\rm pol}(\mathbf{r}) = -\frac{\alpha_0 + \alpha_2 P_2(\cos\theta)}{2r^4}$$

by the equations

$$\alpha_0 = \frac{1}{3}(\alpha_\parallel + 2\alpha_\perp), \quad \alpha_2 = \frac{2}{3}(\alpha_\parallel - \alpha_\perp).$$

From here we obtain $\alpha_0 = 5.258$ a.u., $\alpha_2 = 1.504$ a.u., and from the London formula $C_0 = 49.3$ a.u., $C_2 = 14.1$ a.u.

Although H_2 is not, strictly speaking, a spherically symmetric target, the e^--H_2 and e^+-H_2 interactions can be described, with very good accuracy, in terms of a spherically symmetric potential. The accuracy is improved further when we treat Ps-H_2 collisions. The nonspherical parts of the exchange and the van der Waals potentials are relatively small, and therefore nondiagonal elements of the scattering matrix leading to l transitions are insignificant.

In Fig. 1 we present the cross sections for Ps-H_2 scattering calculated with the HFEGE plus van der Waals potential and compare them with the same calculations where only the spherically symmetric part of both potentials is included. The results are very close. When only the exchange potential is included, the results are practically indistinguishable. We should stress, though, that the only purpose of this calculation is to justify the validity of the approximation of spherical symmetry. The cross sections in this calculation are unphysical because they do not incorporate the Pauli exclusion principle and differ strongly from the more accurate theory.

The approximation of spherical symmetry significantly simplifies the construction of the pseudopotential for Ps scattering. In what follows we outline the version of the pseudopotential used in the present calculations, referring the reader for details to Ref. [5].

The e^--H_2 exchange interaction is incorporated by the pseudopotential

$$V = \sum_{lm} |lm\rangle v_l(r)\langle lm|, \quad (2)$$

where $v_l(r)$ is the spherically symmetric exchange potential in the lth partial wave as a function of the electron radial coordinate r relative to the center of H_2, and $|lm\rangle$ is the projector on the state with angular momentum l and its projection m. This potential can be represented as an integral operator with the kernel

$$V(\mathbf{r},\mathbf{r}') = \frac{1}{r^2}\delta(r - r')\sum_{lm} v_l(r) Y^*_{lm}(\hat{\mathbf{r}}) Y_{lm}(\hat{\mathbf{r}}'). \quad (3)$$

Averaging of this potential over the electron-density distribution in Ps produces the following kernel:

$$V(\mathbf{R},\mathbf{R}') = \sum_{lm}\int \frac{1}{r^2}\delta(r - r') v_l(r) Y^*_{lm}(\hat{\mathbf{r}}) Y_{lm}(\hat{\mathbf{r}}')|\Phi(\boldsymbol{\rho})|^2 d\boldsymbol{\rho}, \quad (4)$$

where $\boldsymbol{\rho}$ is the relative e^--e^+ coordinate, $\mathbf{r} = \mathbf{R} + \boldsymbol{\rho}/2$ and $\mathbf{r}' = \mathbf{R}' + \boldsymbol{\rho}/2$, and $\Phi(\boldsymbol{\rho})$ is the Ps wave function.

The integral (4) can be represented in a form convenient for calculations by going into a coordinate system with the polar axis parallel to the vector $\mathbf{s} = \mathbf{R}' - \mathbf{R}$. We now present the final result, referring the reader for details to [5]:

$$V(\mathbf{R},\mathbf{R}') = \frac{1}{2\pi s}\sum_{ll'}(2l+1)(2l'+1)P_{l'}(\cos\theta_R) \times \int_0^\infty P_l\left(1 - \frac{s^2}{2r^2}\right) P_{l'}\left(-\frac{s}{2r}\right) F_{l'}(r,R) v_l(r) dr, \quad (5)$$

where

$$\cos\theta_R = \frac{R'\cos\Theta - R}{s},$$

Θ is the angle between $\mathbf{R}$ and $\mathbf{R}'$, and $F_l(r,R)$ are coefficients in the expansion

$$e^{-2|\mathbf{r}-\mathbf{R}|} = \sum_{l'=0}^{\infty} F_{l'}(r,R)(2l'+1)P_{l'}(\cos\theta_{\mathbf{rR}}),$$

which can be expressed in terms of the modified spherical Bessel and Hankel functions.

The kernel (5) can be expanded in spherical harmonics,

$$V(\mathbf{R},\mathbf{R}') = \frac{1}{RR'}\sum_{L=0}^{\infty}\frac{2L+1}{4\pi}V_L(R,R')P_L(\cos\Theta).$$

By substitution of this kernel and the spherically symmetric part of the van der Waals potential into the Schrödinger equation, we obtain the following partial radial equation:

$$\frac{1}{2m}\frac{d^2 f_L}{dR^2} + \left[E - \bar{V}_W(R) - \frac{L(L+1)}{2mR^2}\right] f_L(R) - \int V_L(R,R')f_L(R')dR' = 0, \quad (6)$$

where $m = 2$ a.u. is the Ps mass, $\bar{V}_W(R)$ is the spherically symmetric part of the van der Waals potential, and $f_L(R)$ is the radial part of the Ps center-of-mass wave function for the orbital angular momentum L.

B. Calculation of the pseudopotential

The partial potentials $v_l(r)$ in Eq. (2) are all identical to the modified HFEGE potential except for the case $l = 0$. To mock the orthogonality constraint to the occupied σ_g orbital, we use a potential with the repulsive core in the form similar to that used in Ref. [5]:

$$v_0(r) = \frac{B}{r^3}e^{-\beta r}.$$

The fitting parameters B and β are chosen to reproduce the s-wave static-exchange scattering phase shifts for e^--H_2 scattering. Specifically, we choose the static-exchange potential for the e^--H_2 interaction in the form

$$V(r) = V_{st}(r) + v_0(r),$$

where $V_{st}(r)$ is the spherically symmetric part of the static e^--H_2 interaction. One of the best fits was obtained for $B = 5.919$ a.u., $\beta = 0.243\,9$ a.u. The exact and fitted scattering phase shifts are presented in Fig. 2. Due to known deficiencies of the repulsive core pseudopotentials [15], they cannot reproduce *ab initio* phase shifts in a broad energy range. Considering this, the fit looks rather good. We tried slightly different forms of the pseudopotentials and found that the uncertainty in fitting does not affect the Ps-H_2 cross sections.

The modified HFEGE potential is energy dependent; therefore, before using it for Ps-H_2 scattering, we average it over the electron velocity distribution in Ps. For the calculation of the static potential for Ps-H_2 scattering, the HFEGE potential should be averaged further over the electron-density distribution in the position space. This approach might be not quite consistent from the point of view of fundamental quantum mechanics, as the two averages are not correlated. It seems that an average with a correlated distribution in the phase space, like the Wigner distribution [20], should be more appropriate. However, the velocity dependence of the HFEGE potential is very weak. Therefore the inclusion of correlations between position and velocity into the averaging procedure does not change results noticeably. In Fig. 3 we present the exchange potential for several electron velocities and for several Ps velocities obtained from the averaging of the electron potential over the electron velocity distribution in Ps for a given Ps velocity. The potential does not change very much after averaging. Additional checks with the Wigner distribution function for the ground-state Ps [21] show that in the present case a correlated and uncorrelated average leads practically to the same results.

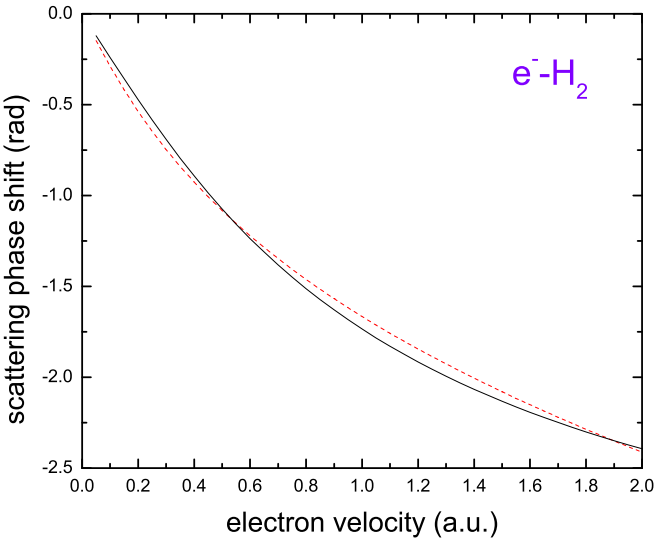

FIG. 2. (Color online) s-wave static-exchange phase shifts for e^--H_2 scattering. Black solid line: *ab initio* calculations with the HFEGE exchange potential. Red dashed line: pseudopotential calculations.

C. Impulse approximation for elastic scattering

The impulse approximation works at higher energies well above the Ps ionization threshold. It appears to be useful in normalizing the pseudopotential calculations because of the uncertainty in the choice of the cutoff parameter R_c in the van

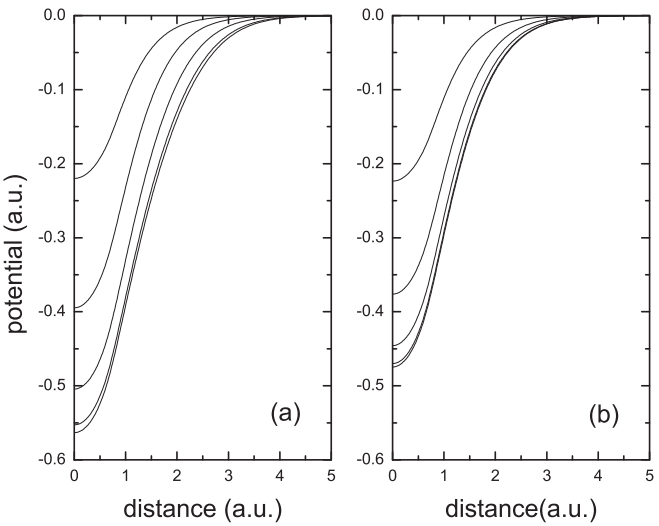

FIG. 3. Local exchange potential for the e^--H_2 interaction. Panel (a): potentials for different electron velocities (from bottom to top), $v = 0.05$, 0.2, 0.50, 1.0, and 2.0 a.u. Panel (b): potential averaged over the electron velocity distribution in Ps for the same Ps velocities as electron velocities in panel (a).

der Waals potential. As in Ref. [5], we attempted to choose R_c by requiring that the pseudopotential calculations merge with the impulse-approximation results at higher velocity (energy).

As in the pseudopotential calculations, we use the approximation of spherical symmetry. The version of the impulse approximation used in the present paper is similar to that used in Refs. [4] and [22], but with a modification related to the on-shell reduction of electron and positron-scattering amplitudes. We start with the electron contribution to the Ps scattering amplitude in the form

$$f(\mathbf{q}) = \int g_f^*(\mathbf{Q}) f^-(\mathbf{v}'',\mathbf{v}') g_i(\mathbf{Q}+\mathbf{q}) d\mathbf{Q}, \tag{7}$$

where $g_i(\mathbf{Q})$, $g_f(\mathbf{Q})$ are initial and final Ps wave functions in the momentum space, $\mathbf{q}$ is the momentum transfer, and f^- is the electron elastic-scattering amplitude as a function of the initial velocity $\mathbf{v}'$ and the final velocity $\mathbf{v}''$:

$$\mathbf{v}' = \mathbf{v}_0 - \mathbf{Q} + \frac{\mathbf{q}}{2}, \quad \mathbf{v}'' = \mathbf{v}_0 - \mathbf{Q} - \frac{\mathbf{q}}{2}, \tag{8}$$

where $\mathbf{v}_0$ is the Ps initial velocity. A similar expression holds for the positron contribution.

The problem with the electron-scattering amplitude entering Eq. (7) is that it is off the energy shell since $|\mathbf{v}'| \neq |\mathbf{v}''|$. The on-shell reduction of Starrett *et al.* [22], also used in Ref. [4], assumes that the amplitude is a function of the effective velocity $v = \max(v', v'')$ and momentum transfer q linked to the electron-scattering angle θ_{sc} by $q = 2v \sin(\theta_{sc}/2)$. In the present application we found that this version of the on-shell reduction might overestimate the contribution of the small scattering angles. Therefore we chose

$$v = \frac{v' + v''}{2},$$

with the same relation between θ_{sc}, q, and v. Although generally different versions of the on-shell reduction can lead to significantly different results for the Ps scattering amplitude, at higher energies they converge, and that serves our major purpose of normalization at higher energies.

D. Binary-encounter approximation for ionization

The impulse approximation can be applied to Ps ionization in its collision with atoms and molecules. There are two difficulties with these calculations. One is related to the aforementioned ambiguity of the on-shell reduction of the electron and positron-scattering amplitudes. The other difficulty is computational. In order to avoid lengthy calculations, Starrett *et al.* [22] used an additional "peaking approximation," assuming that the Ps wave function in the momentum space varies much faster than the scattering amplitude. In fact, one can avoid both difficulties by using a simpler approach based on the binary-encounter approximation [23,24], which employs the differential cross sections for electron and positron scattering, instead of scattering amplitudes.

Consider the process

$$B + \mathrm{Ps} \rightarrow B + e^+ + e^-,$$

where B is a neutral target. The ionization probability due to $e^- - B$ collisions is [23]

$$P_{\mathrm{ion}} = N_B \langle |\mathbf{v} - \mathbf{v}_B| \int_{\Delta E > I} d\sigma \rangle, \tag{9}$$

where $\mathbf{v}_B$ is the relative collision velocity, $\mathbf{v}$ is the electron velocity relative to the Ps center of mass, $d\sigma$ is the differential cross section for $e^- - B$ elastic scattering, and the integration is restricted by the angles which result in the energy transfer to electron ΔE greater than the Ps ionization potential $I = 6.8$ eV. The averaging is over the e^- velocity distribution in Ps. A similar expression can be written for the e^+ contribution. (Interference is neglected.)

By dividing Eq. (9) by the incident flux of particles B, we obtain the total ionization cross section

$$\sigma_{\mathrm{ion}} = \frac{1}{v_B} \langle |\mathbf{v} - \mathbf{v}_B| \int_{\Delta E > I} d\sigma \rangle. \tag{10}$$

In the lab frame where B is at rest, as a result of scattering, the electron velocity changes from $\mathbf{u} = \mathbf{v} - \mathbf{v}_B$ to $\mathbf{u}'$, $|\mathbf{u}'| = |\mathbf{u}|$. The change of the electron kinetic energy in the Ps frame is

$$\Delta E = \frac{1}{2}[(\mathbf{u}' + \mathbf{v}_B)^2 - (\mathbf{u} + \mathbf{v}_B)^2] = \mathbf{v}_B \cdot (\mathbf{u}' - \mathbf{u}).$$

If we direct $\mathbf{v}_B$ along the z axis and introduce spherical angles (θ,ϕ) and (θ',ϕ') for the vectors $\mathbf{u}$ and $\mathbf{u}'$, we obtain

$$\Delta E = v_B u(\cos\theta' - \cos\theta).$$

For the ionization process, integration over θ' is subject to the restriction

$$I < \Delta E < v_B^2,$$

where the upper limit follows from the Ps kinetic energy in the lab frame, consistent with the threshold velocity for the ionization process, $v_B^2 > I$. These constraints correspond to the region in the (θ,θ') plane defined by

$$\cos\theta + \frac{I}{v_B u} < \cos\theta' < \cos\theta + \frac{v_B}{u}. \tag{11}$$

The differential cross section for $e^- - B$ scattering is, assuming that B is spherically symmetric,

$$\frac{d\sigma}{d\Omega} = \sum_{ll'} (2l+1)(2l'+1) f_{l'}^* f_l P_{l'}(\cos\theta_s) P_l(\cos\theta_s),$$

where θ_s is the scattering angle in the lab system, i.e., the angle between $\mathbf{u}$ and $\mathbf{u}'$, and f_l is the partial scattering amplitude

$$f_l = \frac{1 - e^{2i\delta_l(u)}}{2iu}.$$

According to Eq. (10), this expression should be multiplied by $|\mathbf{v} - \mathbf{v}_B| = u$, integrated over scattering angles, and averaged over the velocity distribution of e^- in the ground-state Ps given by

$$\frac{1}{4\pi}|g_{1s}(v^2)|^2 = \frac{1}{4\pi}\frac{256}{\pi(4v^2+1)^4}.$$

For this 5-dim integration we choose the integration variables $\theta,\phi,\theta',\phi',u$. Using the addition theorem for spherical harmon-

ics and writing

$$Y_{lm}(\hat{\mathbf{u}}) = \Theta_{lm}(\cos\theta)\frac{e^{im\phi}}{\sqrt{2\pi}},$$

where $\Theta_{lm}(\cos\theta)$ are normalized associated Legendre functions, we can perform integration over azimuthal angles ϕ and ϕ' with the result

$$\begin{aligned}\sigma_{\rm ion} = {} & \frac{4\pi}{v_B}\int_{I/2v_B}^{\infty} du u^3 \\ & \times \int_{-1}^{1-I/v_B u} d(\cos\theta)|g_{1s}\left(u^2+v_B^2+2uv_B\cos\theta\right)|^2 \\ & \times \sum_{ll'm} f_{l'}^*(u) f_l(u)\Theta_{l'm}(\cos\theta)\Theta_{lm}(\cos\theta) \\ & \times \int_{\cos\theta+I/v_B u}^{\cos\theta+v_B/u} d(\cos\theta')\Theta_{lm}(\cos\theta')\Theta_{l'm}(\cos\theta').\end{aligned} \tag{12}$$

Integration limits follow from the restrictions (11).

E. Calculation of e^- and e^+ potentials and scattering phase shifts

In order to employ the impulse and binary-encounter approximations described above, we need to calculate elastic-scattering phase shifts $\delta_l(u)$ for e^--H_2 and e^+-H_2 collisions. A common method used in describing these processes is to expand the interaction potential in Legendre polynomials [25]:

$$V(\mathbf{r}) = \sum_{\lambda} V_\lambda(r) P_\lambda(\cos\theta), \tag{13}$$

where θ is the angle describing the electron (positron) position in the body frame, relative to the molecular axis. For e^--H_2 scattering the interaction potential consists of a sum of static, exchange, and polarization potentials, and for e^+-H_2 scattering just static and polarization potentials.

For e^--H_2 we have used the static, exchange, and polarization potentials used by Gibson and Morrison [26]. The static potential is calculated from the ground-state H_2 electronic charge density determined by using the wave function of Fraga and Ransil [27]. For e^--H_2 scattering this static potential is attractive, while for e^+-H_2 it is repulsive.

Within the HFEGE model the local exchange potential can also be calculated using the ground-state H_2 electronic charge density. As mentioned above, we use a modified form of this potential called the tuned free electron gas exchange (TFEGE) potential, which has been shown to give good agreement with exact static-exchange calculations for H_2 [9]. In the TFEGE model the ionization potential of H_2 is considered to be an adjustable parameter. By tuning this parameter to 0.071 a.u. instead of the experimental value of 0.564 a.u., good agreement with exact static-exchange calculations is obtained for incident electron energies in the range 0–13.6 eV.

For e^--H_2 scattering the *ab initio* polarization potential of Henry and Lane [28] is used. For e^+-H_2 we have used a spherically symmetric potential of the form

$$V_{\rm pol}(r) = -\frac{\alpha_0}{2r^4}[1-\exp(-(r/r_c)^6)]. \tag{14}$$

We have chosen the value of the cutoff radius to be $r_c = 1.9$ a.u., so that the elastic cross section exhibits a sharp rise as the positron velocity goes to zero and has a magnitude of nearly 1×10^{-16} cm^2 in the energy range 3–7 eV. This agrees with experimental measurements of the e^+-H_2 cross section in this energy range (for example, see Ref. [29]).

If we take the z axis to be along the direction of the molecular axis, we can write the set of coupled equations for the radial wave function of the scattered particle [25]:

$$\begin{aligned}&\left[\frac{d^2}{dr^2}-\frac{l(l+1)}{r^2}-2\langle lm|V|lm\rangle+k^2\right]u_{lm}(r) \\ &\quad = 2\sum_{l'm'}\langle lm|V|l'm'\rangle.\end{aligned} \tag{15}$$

Assuming that the off-diagonal matrix elements are small and can be neglected so that the right-hand side vanishes, we obtain the radial equation

$$\left[\frac{d^2}{dr^2}-\frac{l(l+1)}{r^2}-2\langle l0|V|l0\rangle+k^2\right]u_{lm}(r)=0. \tag{16}$$

Retaining only the first two nonzero terms in the expansion (13), the matrix elements can be written

$$\langle l0|V|l0\rangle = V_0(r)+\frac{l(l+1)}{(2l+1)(2l+3)}V_2(r). \tag{17}$$

Solution of (16) leads to diagonal S-matrix elements in the body frame. By making a rotation to the lab frame [25] we can determine phase shifts for various molecular orientations. We have calculated phase shifts for several orientations and estimated the average over molecular orientation numerically. In all cases the averaged cross sections are very close to cross sections calculated by using only the spherically symmetric term. Therefore we have used phase shifts (up to $l_{\rm max} = 6$) determined by solving Eq. (16), with $\langle l0|V|l0\rangle = V_0(r)$, for use in the impulse and binary-encounter approximations described above.

III. RESULTS AND DISCUSSION

A. e^--H_2 and e^+-H_2 scattering

In Fig. 4 we present the e^- and e^+ phase shifts used in the present paper for calculation of elastic scattering in the impulse approximation and for calculation of ionization cross sections. The cross sections calculated with them agree very well with more sophisticated calculations [26] at low energies and with recommended values [30] derived from combined experimental and theoretical data at higher energies.

We also used the static-exchange s-wave phase shift for e^--H_2 scattering in order to construct the $v_0(r)$ part of the pseudopotential. They are presented in Fig. 2.

B. Ps-H_2 scattering

In Fig. 5 we present the phase shifts for Ps-H_2 scattering calculated with and without account of the van der Waals interaction. The cutoff radius for the van der Waals potential

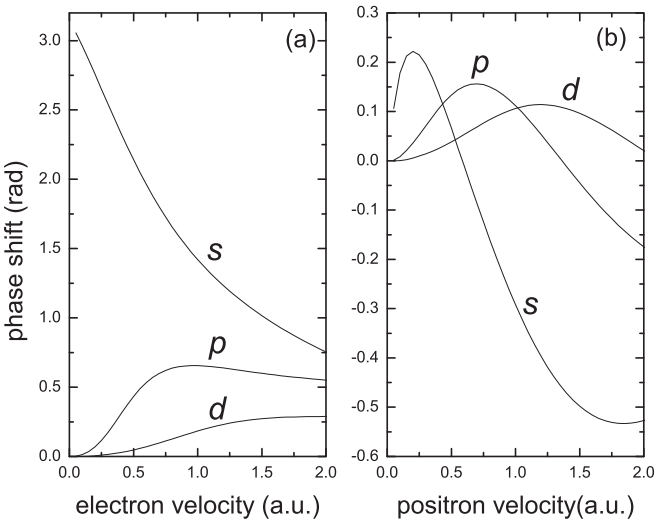

FIG. 4. e^--H_2 and e^+-H_2 scattering phase shifts calculated with the local exchange and polarization potentials.

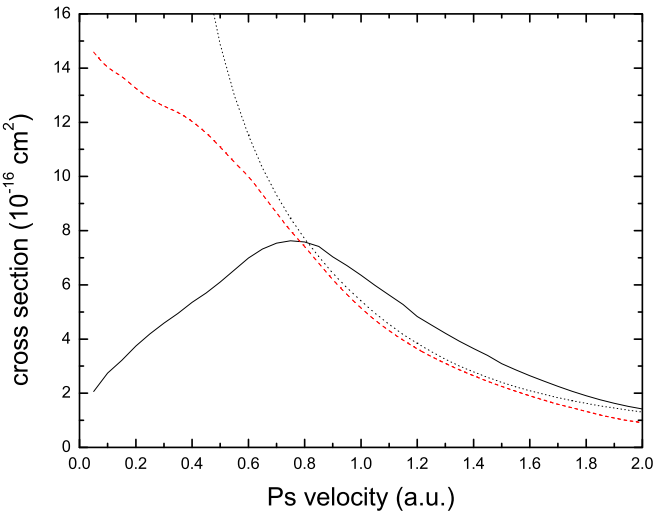

FIG. 6. (Color online) Ps-H_2 elastic-scattering cross sections calculated with account of the van der Waals potential (black solid lines) and without it (red dashed lines). Dotted line: impulse approximation.

was chosen as $R_c = 2.5$ a.u. As shown in Fig. 6, this choice leads to the the pseudopotential cross sections, which are somewhat higher than the results of the impulse approximation in the velocity range between 0.8 and 1.8 a.u., but both curves start to merge at $v = 2$ a.u. The increase of the cutoff radius R_c for the van der Waals potential up to 3.5 a.u. did not lead to a better agreement between the two sets of data. This appears to be different from the results of Ps-Kr calculations [5], where the two curves merge already at $v = 1.5$ a.u., but is consistent with the results for Ps-Ar scattering.

Like in the case of rare-gas atoms, the van der Waals interaction significantly changes the s-wave behavior at low energies and decreases the elastic-scattering cross section. The calculated scattering length for Ps-H_2 scattering is 0.64 and 2.06 a.u., with and without the account of the van der Waals interaction, respectively. The positive sign of the scattering length is an indication of the dominance of the Pauli repulsion, like in the case of rare-gas atoms. The low-energy behavior of the phase shifts follows the threshold laws discussed in Ref. [5].

In Fig. 7 we present the elastic, ionization, and total cross sections for Ps-H_2 scattering and compare them with the elastic and total cross sections for $e^- - H_2$ scattering.

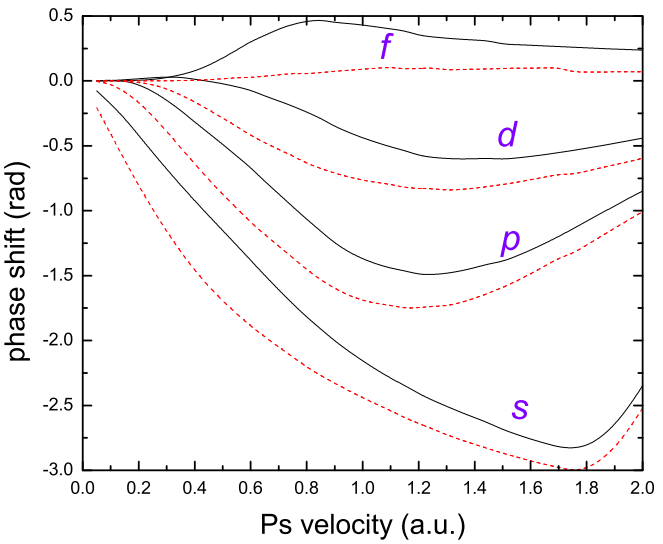

FIG. 5. (Color online) Ps-H_2 scattering phase shifts calculated with account of the van der Waals potential (black solid lines) and without it (red dashed lines).

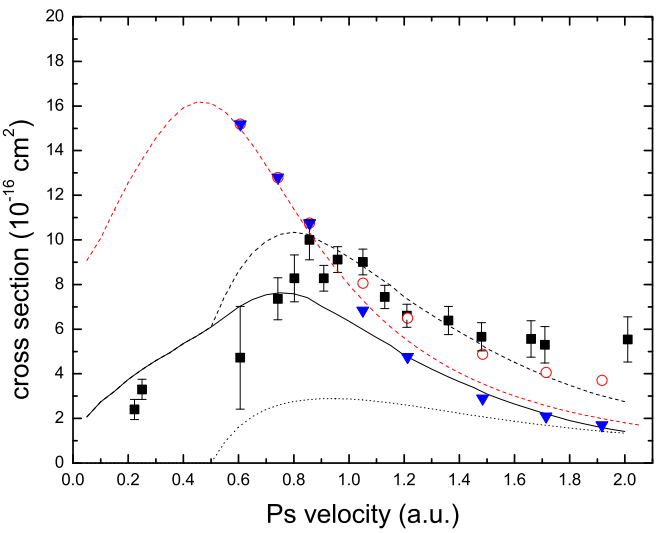

FIG. 7. (Color online) Ps-H_2 and e^--H_2 scattering cross sections. Solid line: elastic Ps-H_2 cross section. Dotted line: Ps ionization cross section. Black dashed line: total Ps-H_2 cross section. Red dashed line: present e^--H_2 elastic cross sections. Error bars: measurements of Skalsey *et al.* [32,33] (low velocities) and Garner *et al.* [31] ($v = 0.6$ a.u. and above). Blue triangles: recommended elastic e^--H_2 cross sections [30]; red open circles: recommended total e^--H_2 cross sections [30]. (Below $v = 1$ a.u. they are the same as those given by the triangles.)

Previous calculations for rare-gas atoms [4,17] showed that the excitation of Ps is negligible compared to the processes of elastic scattering and ionization. Therefore excitation cross sections were not calculated and were not included in the total in the present work. We compare the Ps-H_2 theory with two experiments: the beam experiment of Garner *et al.* [31] measures the total cross section, and the low-energy experiment of Skalsey *et al.* [32,33] extracts the momentum-transfer cross section from the rate of Ps thermalization in a hydrogen gas. The momentum-transfer cross sections are very close to the elastic cross sections at low energies where the measurements were made. Overall, our calculations describe very well the absolute magnitude of the measured total cross section and its dependence on velocity (energy) at velocity below 1.5 a.u. (about $E = 60$ eV). At higher velocities the disagreement might be caused by the failure of the pseudopotential method [15]. This can be seen from the phase shifts shown in Fig. 5: the s phase shift starts to increase at $v > 1.7$ a.u., whereas, to be consistent with the Levinson-Swan theorem [16], it should continue to decrease. On the other hand, the s-wave contribution at high velocities is relatively small.

As in the case of rare-gas atoms, the Ps-H_2 cross section approaches the e^--H_2 cross section plotted as a function of electron velocity at velocities above the Ps ionization threshold. Below this threshold, the Ps-H_2 cross section is significantly lower because of the different nature of the long-range interaction: polarization interaction in e^--H_2 scattering and the van der Waals interaction in Ps-H_2 scattering.

This comparison basically confirms previous conclusions [3] for Ps-H_2 collisions based on experimental results for Ps-H_2 and e^--H_2 scattering. However, some new interesting conclusions can be drawn from the high-velocity region. Although the calculated Ps-H_2 cross section is close to the total e^--H_2 cross section in this region, it is somewhat lower than the experimental results and decreases much faster. (Experimental points give an essentially flat dependence in the velocity range between 1.5 and 2 a.u.). At higher velocities the difference between the elastic and total e^--H_2 (about $2 \times 10^{-16}\,\mathrm{cm}^2$) cross section becomes essential. This difference is mainly due to the H_2 ionization (about $1 \times 10^{-16}\,\mathrm{cm}^2$ at $v = 2$ a.u. [34]) and excitation. The calculated total Ps-H_2 cross sections agree much better with the total e^--H_2 cross sections than with the elastic, although there is no known theoretical justification for this. The general proof [4] of equivalence between the Ps-A and e^--A cross section was given for a structureless target A, and it is not clear why the ionization and excitation processes in e^--H_2 collisions should contribute to the total Ps-H_2 scattering. In addition, the calculated total Ps-H_2 cross section decays faster at high velocities than the total e^--H_2 cross section. This might be due to the failure of the pseudopotential model at higher energies.

A few calculations of the Ps-H_2 collisions were done in the past. Biswas and Adhikari [35,36] used model exchange potential similar to that developed for Ps-He and Ps-H collisions [11] to calculate Ps-H_2 scattering by the coupled-channel method and the Born approximation with exchange. The elastic-scattering calculations were done in the frozen-target approximation, meaning that the van der Waals interaction was not effectively included there. The most recent calculations [36] give the results for total cross sections comparable to ours. However, the composition of this cross section is different from the present. Their total cross section is dominated by Ps ionization and excitation, whereas the elastic cross section is substantially smaller than ours. In contrast, our total cross section is dominated by elastic scattering for energies up to 60 eV. The present ionization cross sections are comparable to those of Biswas and Adhikari, although the latter are about a factor of 2 higher than the present. In addition, Biswas and Adhikari found a significant contribution of excitation of Ps(n) states for the principal quantum number up to $n = 6$, whereas our previous calculations [4] for rare-gas atoms and those of Blackwood *et al.* [17] found these excitations completely negligible. Perhaps the Born approximation, which typically gives large results, caused an overestimation of Ps excitation and ionization in Ref. [36].

Earlier perturbative calculations of Comi *et al.* [37] produced very large elastic cross sections approaching $170 \times 10^{-16}\,\mathrm{cm}^2$ at low energies. This is not surprising, particularly in view of Fig. 1. The elastic cross section is very sensitive to the exchange and van der Waals interactions, and their correct inclusion is crucial. The perturbative approach used in Ref. [37] is certainly not adequate.

IV. CONCLUSION

The pseudopotential method developed earlier for Ps scattering from rare-gas atoms works well also for Ps-H_2 scattering. It also matches reasonably well the results of the impulse approximation at higher velocities (energies). For the Ps ionization cross section we have developed a method based on the binary-encounter approach which avoids the ambiguities of the impulse approximation related to the on-shell reduction of electron- and positron-scattering amplitudes.

Like in the case of rare-gas atoms, the total Ps scattering cross section plotted as a function of Ps velocity is close to e^- scattering cross section above the Ps ionization threshold. At lower velocities the e^--H_2 and Ps-H_2 cross sections are different because of the different nature of the long-range interaction between the projectile and the target, the polarization interaction in the former case and the van der Waals interaction in the latter.

Our calculated total cross sections agree with the swarm measurements at low collision energies and with beam measurements at higher energies. However, there is a noticeable difference with the experiment with regard to behavior of the total cross section at higher velocities: whereas the calculated cross sections continue to decrease with the velocity, the measured cross sections demonstrate essentially flat behavior.

Because of near-spherically-symmetric electron charge distribution in H_2, the approximation of the spherically symmetric potential works quite well for this target. However, for more complicated molecules the methods used in this paper should be extended to potentials with no spherical symmetry.

ACKNOWLEDGMENTS

This work was supported by the National Science Foundation of the United States under Grant No. PHY-1401788.

[1] S. J. Brawley, S. Armitage, J. Beale, D. E. Leslie, A. I. Williams, and G. Laricchia, Science **330**, 789 (2010).
[2] S. J. Brawley, A. I. Williams, M. Shipman, and G. Laricchia, Phys. Rev. Lett. **105**, 263401 (2010).
[3] S. J. Brawley, A. I. Williams, M. Shipman, and G. Laricchia, J. Phys. Conf. Series **388**, 012016 (2012).
[4] I. I. Fabrikant and G. F. Gribakin, Phys. Rev. Lett. **112**, 243201 (2014).
[5] I. I. Fabrikant and G. F. Gribakin, Phys. Rev. A **90**, 052717 (2014).
[6] C. P. Campbell, M. T. McAlinden, F. G. R. S. MacDonald, and H. R. J. Walters, Phys. Rev. Lett. **80**, 5097 (1998).
[7] J. E. Blackwood, M. T. McAlinden, and H. R. J. Walters, Phys. Rev. A **65**, 032517 (2002).
[8] S. Hara, J. Phys. Soc. Jpn. **22**, 710 (1967).
[9] M. A. Morrison and L. A. Collins, Phys. Rev. A **17**, 918 (1978).
[10] P. G. Burke and N. Chandra, J. Phys. B **5**, 1696 (1972).
[11] P. K. Biswas and S. K. Adhikari, Phys. Rev. A **59**, 363 (1999); S. K. Adhikari and P. K. Biswas, *ibid.* **59**, 2058 (1999).
[12] P. K. Biswas and S. K. Adhikari, Chem. Phys. Lett. **317**, 129 (2000).
[13] V. I. Ochkur, Zh. Eksp. Teor. Fiz. **45**, 734 (1963) [Sov. Phys. JETP **18**, 503 (1964)].
[14] M. R. H. Rudge, Proc. Phys. Soc. London **86**, 763 (1965).
[15] J. N. Bardsley, Case Studies At. Phys. **4**, 299 (1974).
[16] P. Swan, Proc. R. Soc. London, Ser. A **228**, 10 (1955).
[17] J. E. Blackwood, M. T. McAlinden, and H. R. J. Walters, J. Phys. B **35**, 2661 (2002); **36**, 797 (2003).
[18] F. London, Trans. Faraday Soc. **33**, 8 (1937).
[19] K. M. Gough, M. M. Yacowar, R. H. Cleve, and J. R. Dwyer, Can. J. Chem. **74**, 1139 (1996).
[20] E. Wigner, Phys. Rev. **40**, 749 (1932).
[21] L. Praxmeyer, J. Mostowski, and K. Wódkiewicz, J. Phys. A **39**, 14143 (2006).
[22] C. Starrett, M. T. McAlinden, and H. R. J. Walters, Phys. Rev. A **72**, 012508 (2005).
[23] B. M. Smirnov, in *The Physics of Electronic and Atomic Collisions*, edited by J. S. Risley and R. Geballe (University of Washington Press, Seattle, WA, 1976), p. 701.
[24] M. R. Flannery, in *Rydberg States of Atoms and Molecules*, edited by R. F. Stebbings and F. B. Dunning (Cambridge University Press, Cambridge, UK, 1983), p. 393.
[25] N. F. Lane, Rev. Mod. Phys. **52**, 1 (1980).
[26] T. F. Gibson and M. A. Morrison, J. Phys. B: At. Mol. Phys. **14**, 727 (1981).
[27] S. Fraga and B. J. Ransil, J. Chem. Phys. **35**, 1967 (1961), see Table II.
[28] R. J. W. Henry and N. F. Lane, Phys. Rev. **183**, 221 (1969).
[29] S. Zhou, H. Li, W. E. Kauppila, C. K. Kwan, and T. S. Stein, Phys. Rev. A **55**, 361 (1997).
[30] A. Muñoz, J. C. Oller, F. Blanco, J. D. Gorfinkiel, and G. Garcia, Chem. Phys. Lett. **433**, 253 (2007).
[31] A. J. Garner, G. Laricchia, and A. Özen, J. Phys. B **29**, 5961 (1996).
[32] M. Skalsey, J. J. Engbrecht, R. K. Bithell, R. S. Vallery, and D. W. Gidley, Phys. Rev. Lett. **80**, 3727 (1998).
[33] M. Skalsey, J. J. Engbrecht, C. M. Nakamura, R. S. Vallery, and D. W. Gidley, Phys. Rev. A **67**, 022504 (2003).
[34] H. C. Straub, P. Renault, B. G. Lindsay, K. A. Smith, and R. F. Stebbings, Phys. Rev. A **54**, 2146 (1996).
[35] P. K. Biswas and S. K. Adhikari, J. Phys. B **31**, L737 (1998).
[36] P. K. Biswas and S. K. Adhikari, J. Phys. B **33**, 1575 (2000).
[37] M. Comi, G. M. Prosperi, and A. Zecca, Phys. Lett. **93A**, 289 (1983).